A Qualitative Comparison Between Two Semiconductor Laser Amplifier Equivalent Circuit Models

A. J. LOWERY

Abstract—**Two different forms of equivalent circuit models have been independently proposed for semiconductor laser amplifiers. These have interesting similarities in their equivalent circuits. This paper will compare the models in terms of derivation, completeness, applications, and computing speed. Results from the transmission line laser model (TLLM) are presented and show the effects of input power, carrier inhomogeneities, and front facet reflectivity on two-input intermodulation distortion.**

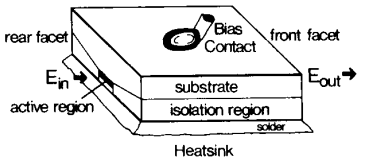

Fig. 1. A typical semiconductor laser amplifier. Note that the facets are usually antireflection coated to avoid passband resonances.

I. Introduction

RECENT publications have shown that the semiconductor laser amplifier (SLA) is becoming a common component in optical communications systems. For example, it can be used as a power booster in optical time-division multiplexed systems [1], [2], a precompensator for fiber dispersion [3], a nonregenerative repeater [4], [5], a duplex repeater [6], an optical preamplifier [7], [8], a wavelength selector [9], an optical switch [10], a bistable element [11], or a pulse shaper [12]. A typical amplifier is shown in Fig. 1.

Despite the large number of different applications, the SLA has a number of undesirable features. These include: the addition of spontaneous emission noise to the signal, nonlinearities due to saturation of the gain, unwanted phase modulation, ripples in the gain spectrum caused by cavity resonances, and polarization sensitivity. It should be noted that some of these features have been used beneficially, e.g., gain saturation can be used for pulse shaping and limiting.

What is clear is that a complete understanding of the processes within the amplifier is required if amplifier designs are to be optimized for specific applications. Computer models may be used to aid this understanding, particularly if they represent the processes in a commonly understood manner; e.g., as electronic components within an equivalent circuit.

Two different proposals for the modeling of amplifiers have been made recently which, although derived in different ways, produce similar equivalent circuits. One method is based on the transmission-line modeling (TLM) method [13] and is a member of a class of models called transmission-line laser models (TLLM's) developed by Lowery in 1987 [14]–[24]. The other method was developed by Saleh in 1988 to aid the understanding of nonlinearities in traveling-wave SLA's [25]. Saleh's method has three variants: 1) the small-signal model, 2) the improved small-signal model, and 3) the large-signal model. This paper refers to the small-signal models unless otherwise stated.

The purpose of this paper is to compare these models in terms of derivation, completeness, variety of applications, and computing speed. Other models, as discussed in [16] will only be commented on where necessary. Quantitative results from the TLLM are given in Section VI.

Manuscript received March 12, 1990.

The author was with the Department of Electrical and Electronic Engineering, University of Nottingham, Nottingham NG7 2RD, England. He is now with the Department of Electrical and Electronic Engineering, University of Melbourne, Parkville, Victoria 3052, Australia.

IEEE Log Number 9036804.

II. Derivations of the Two Models

One common feature of the two models is that they use a time-varying optical field (i.e., electrical field) as their input and output parameters. This allows multicarrier and broad-band input and output waveforms to be modeled. Multiple-carriers occur in wavelength division multiplexed (WDM) and frequency division multiplexed (FDM) systems [25]–[27]. Broad-band inputs occur in most high-bit-rate systems as a consequence of chirping of the laser source and multilongitudinal mode laser oscillation [15]. Fourier transforms may be used to examine the spectra of these waveforms.

A. Solution of the Field Within the Cavity

Both field models are based on a one-dimensional wave equation along the longitudinal axis of the cavity. The transverse and lateral variations in field are ignored with the assumption of a single transverse-lateral mode [14]. However, the methods of solution are different.

TLLM: A transmission-line analogue of the cavity is used, as shown in Fig. 2. This is simply a set of series connected transmission lines, terminated at the facets.

Scattering matrices are placed at the connections between the lines. These represent the optical processes of spontaneous emission, stimulated emission, and attenuation. The optical field is sampled at a rate equal to the propagation delay between the scattering matrices, which is given by the velocity of light and the number of matrices representing the cavity.

Solution consists of passing pulses from scattering matrix to scattering matrix, both in the forwards and backwards directions. When the pulses arrive at a particular matrix, they are operated on, to produce a new pair of pulses, which are in turn passed along the transmission lines. For simplicity, the modeling algorithm requires that all the pulses are synchronized to arrive at all the matrices simultaneously.

The inclusion of both forward and backward traveling waves allows cavity resonances to be modeled. This is because the two waves are coupled at the semireflective facets. The transmission response of such a cavity may be obtained from a Fourier transform of its impulse response. For example, the impulse response for a passive cavity will consist of a series of decaying pulses separated by the round-trip time of the cavity.

SALEH: The wave equation is solved by integration with the approximation that there is no reflection at the cavity facets and, therefore, no cavity resonances. The integration yields the gain and phase shift experienced by a wave passing through the laser cavity [25, (2)]. Both the gain and phase shift are governed by the average carrier density within the guiding (active) region of the SLA, which is modeled with an equivalent circuit.

B. Carrier Density Models

The carrier density is modulated by the use of carriers during the gain process and this causes nonlinearities [26], [27]. Both models derive their equivalent circuits for the carrier density from the carrier density rate equation [28]. However, Saleh's model uses a spatially averaged carrier concentration, whereas the TLLM divides the cavity longitudinally into many separate models. Spatially averaging the carrier concentration requires that an effective value of carrier lifetime, that is constant along the amplifier, should be used. This implies that carrier recombination be approximated to a monomolecular process. Spatial averaging also means that the gain along the amplifier should be set to an average value.

TLLM: The carrier rate equation describes the carrier density dynamics within a section and can be written

$$\frac{dN}{dt} = \frac{I}{qV} - \frac{N}{\tau_s} - S \cdot \frac{ac\Gamma}{\bar{n}_e}(N - N_0) \qquad (1)$$

where N is the carrier density, I is the injection current to the laser, q is the electronic charge, V is the volume of the active region, τ_s is the spontaneous lifetime, s is the average photon density within the section, a is the gain constant (cross section), $c/\bar{n}_e$ is the group velocity of light within the cavity, Γ is the confinement factor of the wave within the active region and, N_0 is the carrier density for transparency.

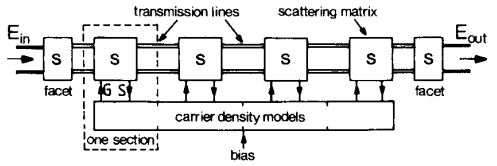

Fig. 2. A transmission-line laser model (TLLM) of a semiconductor laser amplifier composed of scattering matrices (S) coupled by transmission lines.

This equation can be represented by the equivalent circuit shown in Fig. 3 where N is made equivalent to the voltage on the capacitor [14]. This consists of (left–right) a capacitor to represent carrier storage, a current source representing current injection to the laser, a resistor representing spontaneous emission, and a current source representing carrier depletion by stimulated emission. The position of these equivalents mirrors the terms in the equation above.

If the injection current term is time-independent, then this circuit behaves as a low-pass filter, with a time-constant $T = RC$, driven by the stimulated emission term. The stimulated emission is calculated using the average photon density, which is proportional to the square of the input field, i.e.,

$$S = |E|^2 \frac{\bar{n}_e}{Z_p \cdot c \cdot hf} \cdot \frac{\left(\exp\left[a\Gamma(N - N_0)\Delta L\right] - 1\right)}{a\Gamma(N - N_0)\Delta L} \qquad (2)$$

where E is the electric field at the input to a section assuming the field is confined to the active region and is uniform over its cross section [14], Z_p is the transverse wave impedance [14], hf is the photon energy, and ΔL is the section length. Note that the definition of electric field is different to that defined by Saleh; he defines the magnitude of the electric field as simply the square-root of photon density.

The voltage (proportional to charge) on the capacitor representing carrier concentration can then be used to fix the field gain G across a section, length ΔL, using

$$G = a\Gamma \cdot \Delta L \cdot (N - N_0)/2. \qquad (3)$$

One of these equivalent circuits is used for each scattering matrix. This allows inhomogeneities to be accurately modeled [19].

SALEH: Here, the carrier density rate equation is written in terms of the gain deviation from the small-signal gain (small-signal model) or the average-power gain (improved small-signal model). For a constant injection current, the rate equation may then be represented, again, by a low-pass filter driven by a normalized photon density.

C. Representation of the Gain Processes

Both models may be used to find the output field for a given input field. A common feature is the use of a Taylor series expansion of the gain term.

TLLM: The gain process is represented by a series of connected scattering matrices. Many scattering matrices

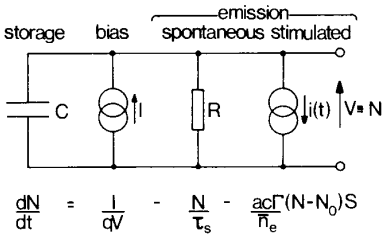

Fig. 3. The equivalent circuit used to model the carrier density rate equation in each section of the transmission-line laser model.

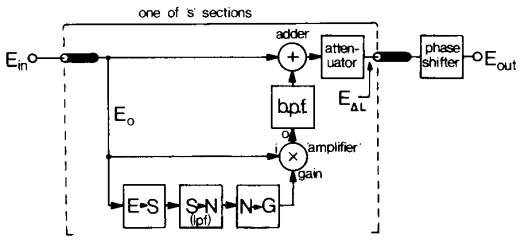

Fig. 4. The transmission-line laser model drawn as an equivalent circuit model. Note that only one wave direction is represented here.

(>2) are used to obtain an accurate large-signal gain model and also to obtain sufficient samples per second of the optical waveform to allow wide-bandwidth input signals to be accepted.

Each scattering matrix is derived from an equivalent circuit of the gain process. It is this equivalent circuit which is remarkably similar to that derived by Saleh. Fig. 4 shows this circuit for one wave direction. Only one scattering matrix's circuit is shown for simplicity. Also shown is a phase-shift element, which will be described later.

How does this circuit relate to the physical process of stimulated emission? To answer this question we have to consider the amplification of the field across a section of length ΔL. This is given by (2) in [25] noting that G is a field gain coefficient in this paper

$$E(\Delta L)/E(0) = \exp\left[G \cdot (1 + j\alpha)\right] \qquad (4)$$

where α is the linewidth enhancement factor [15].

Ignoring the complex part for the moment, as this represents phase modulation which is described later, this equation may be expanded out into a two-term Taylor series, providing the exponent is small, giving

$$E(\Delta L) = E(0) + G \cdot E(0). \qquad (5)$$

The top signal path (Fig. 4) represents the first term on the right-hand side of this equation: $E(0)$. The middle signal path multiplied by the output of the bottom signal path represents the second term in this equation: $G \cdot E(0)$. In reality, G is a function of wavelength. This dependency may be represented, approximately, by a bandpass filter (bpf) placed after the multiplier [14], [18]. Also, the wave may undergo some wavelength independent attenuation, such as by waveguide scattering and free-carrier absorption. These processes are represented by an attenuator placed after the adder.

The bottom signal path calculates the instantaneous photon density ($E \rightarrow S$); then the carrier density ($S \rightarrow N$) and from this, the required gain ($S \rightarrow G$). These blocks represent (2), (1), and (3), respectively. It may be more helpful to think of the multiplier as a voltage controlled amplifier, i.e., the amplification of the optical field is dependent on the carrier concentration.

SALEH: As shown in Fig. 5, Saleh uses only one equivalent circuit to represent the gain along the length of the whole cavity. This produces the problem that the truncated Taylor series becomes inaccurate. To solve this problem, Saleh splits the gain into a constant part (either the unsaturated gain or an average saturated gain) and a modulated part. The constant part is then represented by a multiplier at the input of the circuit leaving the Taylor series derived circuit to represent small variations around the mean gain.

Comparison of Figs. 4 and 5 shows the similarity between the two models. They both include adders, low-pass filters, multipliers, and three signal paths. However, the TLLM has extra components to represent the gain spectrum and constant attenuation. Saleh's model only has one extra component—the linear gain block. Note that some TLLM's also have noise sources to represent spontaneous emission [18].

D. Representation of Phase Modulation

Dynamically-changing phase modulation of the optical carrier across the amplifier's length, caused by the refractive index's dependence on carrier concentration, results in several phenomena in laser amplifiers. For example, rapid changes in phase during fast gain saturation, cause frequency shifts of up to 50 GHz [3].

TLLM: The imaginary part of the gain term in (3) causes phase modulation of the output wave. However, the TLLM equivalent circuits along the cavity do not model this phase modulation. Instead, a single "phase shifter" at the end of the cavity is used, as shown in Fig. 4. The phase shifter is usually modeled by a single variable-length transmission-line stub, coupled to the main cavity. The stub's length l is then modulated by the carrier density, thereby modulating the phase length of the cavity [15].

The change in phase length of the cavity, in radians, is related to the stub's length and the free-space wavelength λ_0 by

$$\theta = 2\pi \cdot l \cdot \bar{n}_e/\lambda_0. \qquad (6)$$

The stub's length is related to the change in index of the active region (*NB not* the effective index of the whole waveguide) Δn, by [15, (10)], noting [29].

$$l = \frac{\Gamma \cdot \Delta n \cdot L}{\bar{n}_e} \qquad (7)$$

where L is the total length of the laser cavity.

Using (13) and (14) from [15] gives the change in phase length, in radians, in terms of change in carrier density in

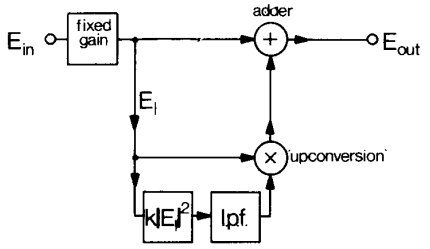

Fig. 5. Saleh's small-signal equivalent-circuit model of a laser amplifier. The fixed (linear) gain is either set to the unsaturated gain or to the mean gain in the modified small-signal model.

the active region ΔN. This is

$$\theta = -\frac{\Gamma a \cdot \Delta N \cdot L \cdot \alpha}{2}. \tag{8}$$

This is consistent with the phase shift produced by the imaginary part of (4), noting that (4) is applied to every section.

Note that the absolute phase length of the cavity, which includes propagation delay, is rarely important. This fact allows the zero-point for phase shift to be arbitrary. However, the propagation delay through the cavity is represented, approximately, by the delays along transmission lines.

SALEH: The imaginary part of the gain term in (4), which causes phase modulation of the optical carrier, remains as a multiplier to the optical field. This multiplication results in phase modulation equal to that modeled by the phase shifter in the TLLM. It is not clear how the imaginary part of the multiplication would be treated in the numerical solution of Saleh's network. The TLLM has a definite advantage in that the output field only ever has a real component, making post-processing much easier.

E. Large Signal Models

Both models suffer from approximating the exponential expansion to a Taylor series. This becomes inaccurate for large arguments.

SALEH: Saleh's small-signal model suffers from the fact that it becomes less accurate as the gain differs from its linear value. To solve this problem, he has also proposed a large-signal model which replaces the Taylor series expansion with a exponential operator. However, he claims that the model is not as suitable for multicarriers.

TLLM: The TLLM uses the Taylor series expansions to provide both the linear (constant) component of the gain and the time-varying gain. This results in a large second term in the Taylor series. To compensate for this, the cavity is divided into sections so that the linear gain per section is small. The accuracy in terms of number of sections is discussed in [14]. However, even a small error was found to give erroneous results when bistability was modeled [16]. For this reason, the model was modified to give the correct gain at the peak of the gain-curve. This entailed modifying (3) to include an exponential operator, giving

$$G = \exp\left(a\Gamma \cdot \Delta L \cdot (N - N_0)/2\right) - 1. \tag{9}$$

Note that, if the band-pass filter is removed, Fig. 4 reduces to the large-signal model derived by Saleh.

TABLE I
COMPARISON BY NUMBER OF PARAMETERS

Parameter	TLLM	Saleh
Multicarrier inputs	Yes	Yes
Broad-band inputs	Yes	Yes
Gain versus carrier density	Yes	Yes
Confinement factor	Yes	Yes
Transparency carrier density	Yes	Yes
Gain spectrum	Lorentzian	Flat
Reflective facets	Yes	
Backward waves	Yes	
Spontaneous emission	Yes	
Bias modulation	Yes	Possible
Attenuation	Yes	Included in gain
Carrier inhomogeneity	Longitudinal	Spatial average
Longitudinal photon inhomogeneity	Longitudinal	Spatial average
Propagation delay	Yes	
Dynamic phase shift	Yes	Yes
Recombination mechanisms	Monomolecular, bimolecular, and Auger	Effective monomolecular approximation
DFB grating	Yes [31]	
Internal reflections	Yes [31]	
Multiple contacts	Yes	
Nonlinear gain	Possible	Possible

TABLE II
COMPARISON BY APPLICABILITY

Application	TLLM	Saleh
Cavity resonances	Yes	
Traveling-wave SLA's	Yes	Yes
Near-TW SLA's	Yes	
Fabry-Perot SLA's	Yes	
Unsaturated gain	Yes	Yes
Saturated gain	Dynamic	Steady-State (S, M)[a] Dynamic (L)
Pulse compression	Yes	Yes (L only, see [20])
Noise saturation of gain	Yes	
Noise power	Yes	Could be added
Noise spectrum	Yes	Flat
Duplex operation	Yes	
Two-color saturation	Yes	Yes
Bistability	Yes	
Intermodulation	Yes	Yes
Crosstalk	Yes	Yes
Asymmetric gain	Yes	Yes
Gain versus wavelength	Yes	
Self-phase modulation	Yes	Yes

[a] S = small-signal model, M = modified small-signal model, L = large-signal model.

III. Model Completeness

One criterion for the assessment of numerical models is how many parameters that they can deal with. This should, of course, be offset against the complexity of the

algorithm, the ease of understanding, and the computational effort for a standard problem.

Table I summarizes the models' completeness in terms of a number of parameters. In some cases, the models could be easily modified to include the parameter.

IV. Applicability

The number of different applications for which the models are valid is somewhat dependent on the number of parameters modeled. Table II lists some common applications of SLA models together with which modeling approach is suitable.

Not that Saleh's model does not include backward waves. This precludes the modeling of amplifiers with reflective facets such as near-traveling-wave amplifiers and Fabry–Perot amplifiers. In particular, bistability cannot be modeled [11], [16]. Also, Saleh's model does not include distributed noise sources representing spontaneous emission. Although these could be added, the gain saturation caused by spontaneous emission could not be calculated [30].

V. Computational Task

A small computational task means that a model is much more suitable for optimizing a design. However, accuracy is nearly always traded for simplicity.

TLLM: This uses many more, more complex, equivalent circuits to model the cavity than Saleh's model. Therefore, the computational task per iteration will be increased by at least the number of model sections.

The other important factor is the iteration timestep ΔT. For TLLM's this is related to the number of sections s, the cavity length L, and the group velocity $c/\bar{n}_e$, by [14]

$$\Delta T = L\bar{n}_e/cs. \tag{10}$$

Note that the sampling rate of the optical field is well below the optical frequency. This is possible because the linewidth of the amplifier's input signal is usually small.

The number of sections s is usually between 10 and 100. This gives iteration timesteps in the range of 10 fs to 1 ps for most devices. Thus, many iterations may be needed if the low-frequency characteristics of amplifiers are to be studied. It is clear from (10) that a small number of sections will reduce the computational task considerably. However, s affects both the Taylor series accuracy, as discussed, and the bandwidth of the model. A high bandwidth is important if very short pulses or multiple-carrier inputs are to be modeled. The bandwidth is given by $1/(2\Delta T)$. Alternatively, the bandwidth is given by s multiplied by the free-spectral range of the laser cavity.

Having a large number of sections also improves the modeling of carrier and photon inhomogeneities. This is important in ultrashort (a few ps) pulse amplification. However, the use of an expression for average photon density and the assumption of a homogeneous carrier density is sufficiently accurate for longer pulses [19].

SALEH: It is not clear what the sampling rate in these models should be. However, it is probable that the linewidth of the output wave is the main consideration. This means that the sampling rate is potentially much lower than in the TLLM, except for broadly-spaced multicarrier inputs. Together with the fact that only one equivalent circuit is used, this should give a computational speed increase of more than 100× over the TLLM.

VI. Examples of a TLLM for Intermodulation

This section shows how the TLLM may be used to assess intermodulation distortion in a laser amplifier with parameters as given in Table III. The laser cavity was divided into four model sections, giving a timestep of 1.666 ps. The four-section model was run for 4096 iterations and a 2048 point transform was taken after 2048 iterations. This allowed the carrier density to settle to its steady-state value before the spectrum was examined. The input was two optical carriers, of equal power and spaced at 585.93 MHz and placed near the center of the modeled bandwidth.

A. Intermodulation Versus Input Power

The output spectrum was examined for a series of input powers, from 5 to 700 μW, with the assumption of zero facet power reflectivities. Fig. 6 plots gain and the output powers of the carriers and all significant intermodulation products relative to the total output power. At low input powers the upper and lower frequency carriers are of equal output magnitude, each comprising half of the total output power. However, as the input power per carrier is increased, the lower frequency carrier becomes dominant. This effect is due to phase modulation of the carriers and was observed by Webb and Hodgkinson at carrier spacings close to the reciprocal of carrier lifetime [32]. As the input power is increased, the number and amplitude of the intermodulation products (marked "1" to "4", corresponding to the number of frequency spacings away from the carriers) increases. The gain also starts to saturate. Dominance of the lower frequency sidebands over the corresponding upper frequency sidebands is seen at higher powers. These results are broadly in agreement with those of Webb and Hodgkinson.

B. Intermodulation Versus Number of Model Sections

The use of more model sections allows for better representation of inhomogeneities in gain and carrier density and studies showed that less saturation of the amplifier occurred when more sections were used. Fig. 7 illustrates the effect of the number of sections on the accuracy of the simulations by plotting the carrier and intermodulation product levels against the number of model sections with an input power of 100 μW per carrier. The number of iterations was increased in proportion to the number of sections to maintain the transform resolution. The intermodulation product levels decrease with number of sections, indicating that models assuming a homogeneous gain (e.g., Saleh's) may overestimate intermodulation distortion. Also, the difference in carrier output levels diminishes with number of sections. The four-section model used in Sections VI-A and VI-B overestimated the second sideband levels by about 3 dB.

TABLE III
PARAMETERS OF THE MODELED DEVICE

Symbol	Parameter	Value	Unit
λ_0	Wavelength	1500	nm
L	Cavity Length	500	μm
w	Cavity Width	1.5	μm
d	Cavity Depth	0.15	μm
$\bar{n}_e$	Group Effective Index	4.0	
a	Gain Cross Section (dg/dN)	2.7×10^{-16}	cm^2
Γ	Confinement Factor	0.3	
N_0	Transparency Carrier Density	9.0×10^{17}	cm^{-3}
τ_s	Carrier Lifetime	400	ps
α	Linewidth Enhancement Factor	5.6	
α_{sc}	Scattering Attentuation Factor	40.0	cm^{-1}
G_u	Unsaturated Gain	10.0	dB

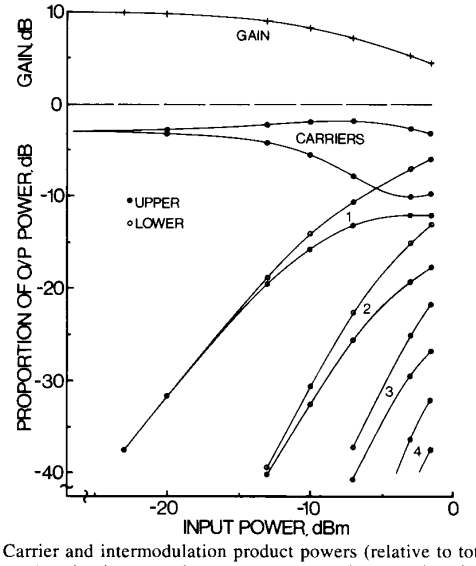

Fig. 6. Carrier and intermodulation product powers (relative to total output power) and gain versus input power per carrier. Labels refer to the IMP's displacement from the carriers.

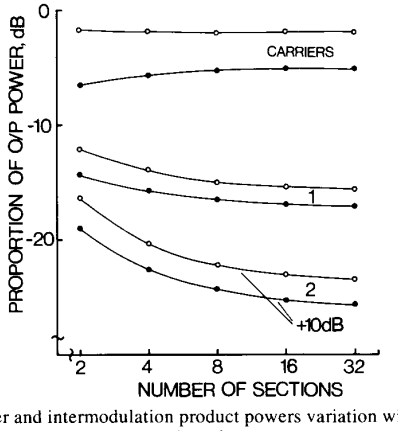

Fig. 7. Carrier and intermodulation product powers variation with number of model sections.

C. Intermodulation Versus Front Facet Reflectivity

Mukai and Yamamoto, among others, have calculated that a high reflectivity front facet may be used to lower the noise figures of laser amplifiers [33]. A series of simulations was carried out to find the effect of a front facet reflectivity on intermodulation. The rear facet was made nonreflective to prevent cavity resonances filtering the intermodulation products and thus producing central-wavelength dependent results.

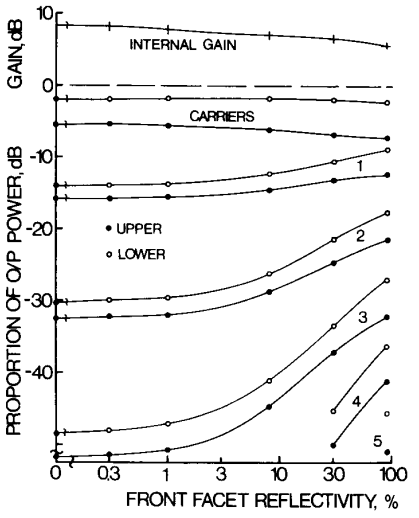

Fig. 8. Carrier and intermodulation product power variation with front facet reflectivity. Internal gain is also plotted.

Fig. 8 shows the relative powers of the carriers and intermodulation products versus front facet reflectivity over a range of 0 to 90% reflectivity at an input power of 100 μW per carrier. Also shown is the variation of internal gain (i.e., neglecting power loss at the front facet) with reflectivity. Facet reflectivities below 1% have little effect on intermodulation distortion, though the use of higher gain amplifiers many increase the distortion. However, at 30% reflectivity, the first set of sidebands are increased by about 3 dB. Other sidebands suffer from much greater increases in power. This increased intermodulation distortion is a result of increased carrier density modulation caused by the backward-traveling wave. This wave also causes increased gain saturation.

VII. Discussion and Conclusion

This paper has compared two models of semiconductor laser amplifiers which both use equivalent circuits to determine the amplifier's output field in terms of the input field. Although this paper does not include quantitative comparisons of the two models, it does provide useful measures by which the models may be assessed. These include the number of parameters that may be considered, the variety of applications and the computation speed for a particular problem.

This paper also shows that similar algorithms may be derived in different ways. The transmission-line laser model was developed by considering the physical processes within the laser. Saleh developed his models by mathematical manipulation of standard equations before developing equivalent circuits.

Such a comparison exercise is useful because it verifies the validity of the models, particularly as the models were

derived independently. It can also point to new applications for the models. For example, the similarity between the models indicated that the TLLM could be used for the modeling of nonlinearities in multicarrier systems.

Also, comparison may also lead to some degree of cross fertilization, leading to a hybrid model. For example, the removal of a constant linear gain from the Taylor series expansion in the TLLM may be useful in flat gain-spectrum models. On the other hand, Saleh's model may benefit from the TLLM's phase model. This would remove the need for a complex multiplication.

The purpose of this paper was not to support a particular model and deride the other. Both models offer advantages for some applications. In general, however, the TLLM is more flexible. However, this is at the cost of a complex algorithm and a large computational task. Both models aid understanding of nonlinearities in laser amplifiers.

The intermodulation distortion simulations using the TLLM showed that modeling inhomogeneities in gain along the cavity reduced intermodulation distortion. Facet reflectivities above 1% were shown to increase intermodulation distortion. These two examples showed the advantage of using a TLLM over Saleh's model: the disadvantage being the increased computational effort required by the TLLM.

Acknowledgment

The author would like to thank J. Williams for running the numerical simulations.

References

[1] J. M. Weisenfeld, G. Eisenstein, R. S. Tucker, G. Raybon, and P. B. Hansen, "Distortionless picosecond pulse amplification and gain compression in a travelling-wave InGaAsP optical amplifier," *Appl. Phys. Lett.*, vol. 53, pp. 1239–1241, 1988.

[2] R. S. Tucker, G. Eisenstein, S. K. Korotky, L. L. Buhl, J. J. Veselka, G. Raybon, B. L. Kasper, and R. C. Alferness, "16 Gbit/s fibre transmission experiment using optical time-division multiplexing," *Electron. Lett.*, vol. 23, pp. 1270–1271, 1987.

[3] N. A. Olsson, G. P. Agrawal, and K. W. Wecht, "16 Gbit/s, 70 km pulse transmission by simultaneous dispersion and loss compensation with 1.5 μm optical amplifiers," *Electron. Lett.*, vol. 25, pp. 603–605, 1989.

[4] M. G. Oberg, N. A. Olsson, L. A. Koszi, and G. J. Przybylek, "313km transmission experiment at 1Gbit/s using optical amplifiers and a low-chirp laser," *Electron. Lett.*, vol. 24, pp. 38–40, 1988.

[5] A. J. Lowery, "A comparison between Fabry-Perot and travelling wave laser amplifiers in an 8 Gbps repeated optical system using a time-domain model," *J. Phys. D—Appl. Phys.*, vol. 21, pp. S177–S179 (ECOOSA88 Special Edition), 1988.

[6] H. J. Westlake, and M. J. O'Mahony, "Bidirectional and two-channel transmission system measurements using a semiconductor-laser-amplifier repeater," *Electron. Lett.*, vol. 23, pp. 649–651, 1987.

[7] I. W. Marshall and M. J. O'Mahony, "10 GHz optical receiver using a travelling-wave semiconductor laser preamplifier," *Electron. Lett.*, vol. 23, pp. 1052–1053, 1987.

[8] N. A. Olsson, M. G. Oberg, L. D. Tzeng, and T. Cella, "Ultra-low reflectivity 1.5μm semiconductor laser preamplifier," *Electron. Lett.*, vol. 24, pp. 569–570, 1988.

[9] M. P. Vecchi, H. Kobrinski, E. L. Goldstein, and R. M. Bulley, "Wavelength selection with nanosecond switching times using distributed feedback optical amplifiers," in *Proc. ECOC '88, IEE Conf. Pub. 292*, Pt. 1, Brighton, Eng., pp. 247–250, 1988.

[10] M. J. Adams, "Twin-stripe laser amplifier switch," in *Proc. ECOC '88, IEE Conf. Pub. 292*, Pt. 1, Brighton, England, pp. 324–327, 1988.

[11] K. Otsuka and S. Kobayashi, "Optical bistability and nonlinear resonance in a resonant-type semiconductor laser amplifier," *Electron. Lett.*, vol. 19, pp. 262–263, 1983.

[12] I. W. Marshall, and D. M. Spirit, "Observation of large pulse compression by a saturated travelling wave semiconductor laser amplifier," Presented at CLEO '88, Anaheim, CA, paper TuM64.

[13] W. F. R. Hoefer, "The transmission-line matrix method—Theory and applications," *IEEE Trans. Microwave Theory Tech.*, vol. MTT-33, pp. 882–893, 1985.

[14] A. J. Lowery, "A new dynamic semiconductor laser model based on the transmission line modelling method," *IEE Proc. J., Optoelectron.*, vol. 134, pp. 281–289, 1987.

[15] ——, "A model for picosecond dynamic laser chirp based on the transmission line laser model," *IEE Proc. J., Optoelectron.*, vol. 135, pp. 126–132, 1988.

[16] ——, "New inline wideband dynamic semiconductor laser amplifier model," *IEE Proc. J, Optoelectron.*, vol. 135, pp. 242–250, 1988.

[17] ——, "Explanation and modelling of pulse compression and broadening in travelling-wave laser amplifiers," *Electron. Lett.*, vol. 24, pp. 1125–1126, 1988.

[18] ——, "A new time-domain model for spontaneous emission in semiconductor lasers and its use in predicting their transient response," *Int. J. Numer. Modelling*, vol. 1, pp. 153–164, 1988.

[19] ——, "Modelling ultra-short pulses (less than the cavity transit time) in semiconductor laser amplifiers," *Int. J. Optoelectron.*, vol. 3, pp. 497–508, 1988.

[20] ——, "Pulse compression mechanisms in semiconductor laser amplifiers," *IEE Proc. J; Optoelectron*, vol. 136, pp. 141–146, 1989.

[21] ——, "A new dynamic multimode model for external cavity semiconductor lasers," *IEE Proc. J, Optoelectron*, vol. 136, pp. 229–237, 1989.

[22] ——, "A new time-domain model for active mode-locking based on the transmission-line laser model," *IEE Proc. J, Optoelectron*, vol. 136, pp. 264–272, 1989.

[23] ——, "Cyclic three-phase amplitude jitter in mode-locked semiconductor lasers," *Electron. Lett.*, vol. 25, pp. 799–800, June 1989.

[24] A. J. Lowery and I. W. Marshall, "Stabilisation of mode-locked pulses using a travelling-wave semiconductor laser amplifier," *Electron. Letts.*, vol. 26, pp. 104–106, Jan. 1990.

[25] A. A. M. Saleh, "Non-linear models of travelling-wave optical amplifiers," *Electron. Lett.*, vol. 24, pp. 835–837, 1988.

[26] T. E. Darcie and R. M. Jopson, "Non-linear interactions in optical amplifiers for multifrequency lightwave systems," *Electron. Lett.*, vol. 24, pp. 638–640, 1988.

[27] R. M. Jopson, T. E. Darcie, K. T. Gayliard, R. T. Ku, R. E. Tench, T. C. Rice, and N. A. Olsson, "Measurement of carrier density mediated intermodulation distortion in an optical amplifier," *Electron. Lett.*, vol. 23, pp. 1394–1395, 1987.

[28] M. J. Adams and M. Osinski, "Longitudinal mode competition in semiconductor lasers: Rate equations revisited," *IEE Proc. I, Solid State and Electron Devices*, vol. 129, pp. 271–274, 1982.

[29] A. J. Lowery, Errata, *IEE Proc. J.: Optoelectron.* vol. 135, p. 297, 1988.

[30] L. Thylén, "Amplified spontaneous emission and gain characteristics of Fabry-Perot and traveling wave type semiconductor laser amplifiers," *IEEE J. Quantum Electron.*, vol. QE-24, pp. 1532–1537, 1988.

[31] A. J. Lowery, "Dynamic modelling of distributed-feedback semiconductor lasers using scattering matrices," *Electron. Lett.*, vol. 25, pp. 1307–1308, Sept. 1989.

[32] R. P. Webb and T. G. Hodgkinson, "Experimental confirmation of laser amplifier intermodulation model," *Electron. Lett.*, vol. 25, pp. 491–493, Apr. 1989.

[33] T. Mukai and Y. Yamamoto, "Noise in an AlGaAs semiconductor laser amplifier," *IEEE J. Quantum Electron.*, vol. QE-18, pp. 564–575, 1982.

A. J. Lowery, photograph and biography not available at the time of publication.